17th World Conference on Earthquake Engineering, 17WCEE
Sendai, Japan - September 13th to 18th 2020

DYNAMIC EFFECT OF NONSTRUCTURAL EQUIPMENTS AND MASS RATIO ON THE MAIN STRUCTURE

Q. Pan [1], B. Huang [2], S. Günay [3], W. Lu [4]

[1] *Graduate Student, College of Civil Engineering, Nanjing Tech University, Nanjing China. panqihao@njtech.edu.cn*
[2] *Associate Professor, College of Civil Engineering, Nanjing Tech University, Nanjing China. baofeng@njtch.edu.cn*
[3] *Project Scientist, Pacific Earthquake Engineering Research Centre, University of California, Berkeley CA USA. selimgunay@berkeley.edu*
[4] *Professor, College of Civil Engineering, Tongji University, Shanghai China, wally@tongji.edu.cn*

Abstract

Seismic damage to equipment installed in residential, commercial, hospital, and multistory industrial buildings are reported in major earthquakes that happened in the past decades. Equipment, such as heating, ventilation, air conditioning systems, etc. are attached to the building structure as the nonstructural system which experiences the inertia force or deformation action transferred from the main building. Mass of these equipment are comparatively smaller than the main structure, therefore the resulting inertia force is neglected in seismic design of the building structure. However, the mass of heavy equipment, such as the cooling tower, water pump assembly, medical air unit, etc., cannot be ignored in the seismic design of the main structure. The mass ratio (MR, the mass of the equipment divided by the total mass of the structure) is one of the important parameters to determine the dynamic interaction between the equipment and the main structure.

In this study, to investigate the seismic interaction in terms of the MR, a 1/10 scaled 4-story steel moment frame was built following the similitude law such that the dynamic response of this frame can be derived to that of the prototype. To compute the dynamic characteristics of the frame, it was simplified as a four degree-of freedom (4DOF) system. The equivalent masses of the equipment were applied to various floor levels ignoring the stiffness and damping of the equipment. The relationship between the MR and vibration period of the system was obtained by solving the corresponding eigenvalue problem. To verify the accuracy of the simplified model, finite element models were constructed with OpenSees and SAP2000. The resulting vibration period was observed to match that of the closed-form solution. Free vibration tests were employed and the vibration period and damping ratios of the frame were computed based on the experimental results. In the same mass assignment scenario, the vibration period from the closed-form solution was identical to that from the experiment. The relationships between the mass ratio, damping ratio, and the fundamental vibration period were discussed based on the experimental results.

Keywords: Equipment; interaction; vibration period; damping ratio; dynamic response.

1. Introduction

Mechanical and electrical equipment such as sprinkler systems, switchgear, and transformers, etc. are the functional utilities in building structures. They play a critical role in ensuring a proper living and working environment for occupants of the building. In strong earthquake excitations, the resulting failure of such equipment is likely to disrupt the post earthquake response and recovery (Caldwell et al. 2007 [1]). Moreover, historical earthquakes have demonstrated that electrical equipment as a whole are often not adequately restrained and/or anchored, which can lead to significant damage due to overturning and/or sliding. In the 27 May 1964 Great Alaska earthquake, mechanical systems like liquid tanks, elevators, boilers, etc. were damaged severely in downtown Anchorage (Ayres et al. 1967 [2]). There were no available seismic design guidelines for the mechanical facilities to follow at that time. As a result of severe earthquake shaking, medical facilities in Los Angeles Olive View Medical Center were damaged significantly in 9 February 1971 San Fernando earthquake (Lew et al. 1971, Ayres and Sun 1973 [3,4]). This building was demolished after this earthquake, and a new building was built in the same place in 1980s. During the 17 January 1994 Northridge earthquake, only slight equipment damage was experienced because of the supporting brackets failure (OSHPD 1996 [5]). High-tech industry is usually equipped with data processing equipment being supported by the steel racks, cabinets, etc. where seismic damage was reported in the 17 October 1989 Loma Prieta earthquake (Ding et al. 1990 [6]). In the 12 January 2010 Haiti earthquake, many electrical equipment in building structures were damaged as a result of unqualified restraints or anchors (Goodno et al. 2011 [7]). Counterweight and cab derailments, guide rail damage, jammed doors, and shifted equipment occurred in half of the investigated buildings (Miranda et al. 2012 [8]). Measures should be taken to improve the seismic performance of these equipment.

As one type of nonstructural component (NC), the mechanical and electrical equipment is not designed to carry the seismic load of the main structure. In fact, the immediate load they experience is transferred from the connections between the equipment and the main structure (Chen and Soong 1988, Villaverde 1997 [9,10]). As a result of the dynamic and physical characteristics of the two systems such as the vibration period, mass, and damping ratio, the interaction of the two systems may influence their seismic performance. Floor response method is typically employed to evaluate the seismic performance of the equipment under the floor motion excitation. The pioneer work of Penzien and Chopra has been carried out to generate the peak response of the NCs [11]. A simplified analytical two-degree-of-freedom (2DOF) model was built to investigate the equipment-structure interaction (Igusa et al. 1985 [12]). Using similar method, multiply supported NCs were studied regarding the interaction performance ([13,14]). The amplification effect was considered in the lower floors when the natural period of the NCs was equal to the 2nd or 3rd period of the main structure with the consideration of the nonlinearity and narrowband excitation of the primary structure [15]. In Segal and Hall [16], it was observed that mounting of equipment on the main structure would not reduce the peak response and it would not act as a damper for the main structure. Using the structure interaction, an accurate prediction for the top displacement of the NC was achieved by considering the relationship between the interacting force and the response under dynamic loading [17]. Because NCs are not subjected to the external excitation, but they are excited by the inertia force induced by the main structure, resulting NC response can be considered in the terms of floor response [9]. However, limited work in literature investigates the interaction effect on the mass ratio of the equipment (or NCs) to the main structure.

In the current study, to investigate the contribution of the mass ratio on the dynamic properties of the equipment-main structure system, a scaled 4-story steel building was constructed in the lab. Additional steel plates representing the mass of the equipment were fixed in different floor levels. Finite element model (FEM) was created to compute the dynamic parameters of the structure-equipment system. To evaluate the analytical results, free vibration tests were performed to obtain the experimental dynamic parameters. The dynamic effect of the mass of the equipment on the main structure are elaborated based on the experimental and analytical results.

2. Test Specimen

A 4-story, one-bay symmetric steel building, with a span, story height and total height of 6.0m, 4.5m and 18.0 m, was chosen to be the prototype building structure to support the equipment (Fig. 1). The floor of each story is made of reinforced concrete. Due to the limitation of the experimental facilities, the building was scaled down to 10% of the prototype structure. The building was designed following the current Chinese seismic code ([18]). To calibrate the horizontal stiffness of the structure, diagonal braces with double L-shape steel were manufactured. All the joints are connected with bolts so that the whole building can be fabricated easily (Fig. 1c). The concrete slab was replaced with steel grid in the scaled structure. The detailed geometrical and structural parameters are listed in Table 1. As a result of the limited construction materials in real world, if the same materials were used in the two structures, the scaled building structure would lead to the distortion of the mass, and structural response such as the deformation, acceleration, stress, etc. Therefore, additional mass representing the equipment is needed to be placed on each floor based on similitude law (Kim et al. 2009, [19-22]). According to the theory of similitude introduced in [21], the resulting conversion coefficients between the prototype and the scaled structure are shown in Table 2. They can be applied to convert the dynamic responses of the scaled structure to those of the prototype structure.

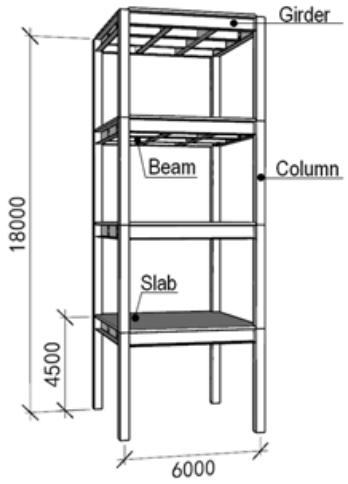

a). Prototype (unit: mm)

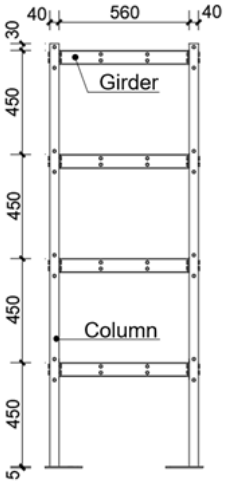

b). Elevation view of the down-scale structure (unit: mm)

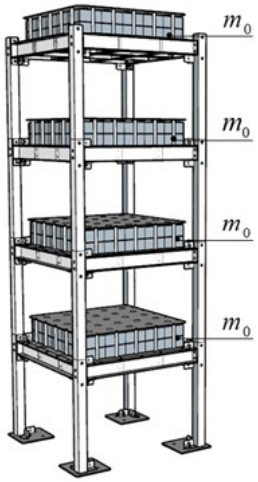

c). Completed structure with additional masses

Fig. 1. Test specimen

Table 1. Parameters of the Test Specimen.

Item	Prototype		Scaled
Height (m)	18.0		1.8
Mass of floor (kg)	81,129.3		45.1
Mass of equipment (kg)	36,000.0		766.2
Column	Height (m)	4.5	0.45
	Cross Section (mm)	Steel pipe 400×400×20	Steel pipe 40×40×2
Beam	Length (m)	5.6	0.56
	Cross Section (mm)	C-shape steel 600×300×25	C-shape steel 60×30×2.5

Table 2. Conversion Coefficient.

Property	Physical Parameter	Conversion Coefficient
Geometrical	Length	0.1
	Strain	1.00
	Elastic modulus	1.00
Material	Stress	1.00
	Density	10.0
	Mass	0.01
Load	Concentrated force	0.01
	Linear load	0.1
	Surface load	1.0
	Moment	0.001
Dynamic	Period	0.316
	Acceleration	1.00
	Time	0.316

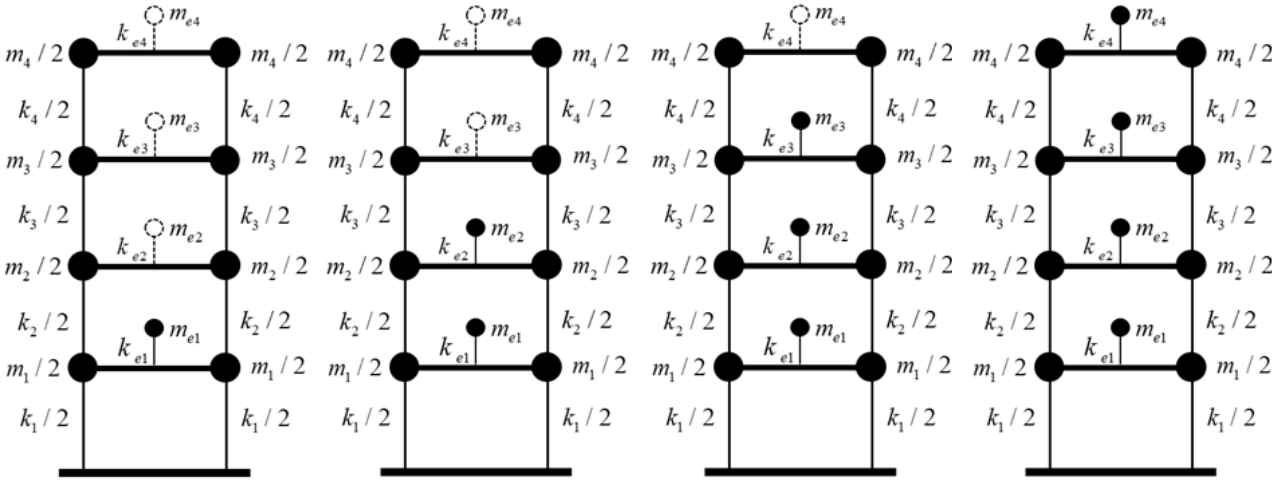

a). Equipment in one floor b). Equipment in two floors c). Equipment in three floors d). Equipment in four floors

Fig. 2. Four degree of freedom model including the equipment modeling

3. Numerical Analysis

3.1 Building without equipment

The dynamic properties, especially the vibration frequencies, are fundamental characteristics representing the influence of the mass of the equipment on the main structure. Prior to application of the mass of the equipment on the main structure, the vibration frequency should be known such that the mass ratio effect can be analyzed properly. To compute the vibration frequency of the 3D structure, it is simplified as a 4DOF system with four lumped mass at each story level (Fig. 2). The equation of motion of this system for free vibration (Chopra 2012 [23]) is shown in Eq. (1) below:

$$M \begin{Bmatrix} \ddot{\iota}_1 \\ \ddot{\iota}_2 \\ \ddot{\iota}_3 \\ \ddot{\iota}_4 \end{Bmatrix} = \mathbf{0} \tag{1}$$

where, $M=\begin{bmatrix} m_1 & 0 & 0 & 0 \\ 0 & m_2 & 0 & 0 \\ 0 & 0 & m_3 & 0 \\ 0 & 0 & 0 & m_4 \end{bmatrix}$ is the mass matrix; $K=\begin{bmatrix} k_1+k_2 & -k_2 & 0 & 0 \\ -k_2 & k_2+k_3 & -k_3 & 0 \\ 0 & -k_3 & k_3+k_4 & -k_4 \\ 0 & 0 & -k_4 & k_4 \end{bmatrix}$ is the stiffness matrix; u_i, $\dot{i}$, and $\ddot{}$ (i = 1, 2, 3, 4) are the displacement, velocity, and acceleration of the ith mass; Rayleigh damping is used so that the damping matrix $C=a_0M+a_1K$ is the damping matrix with $a_0=\zeta\frac{2\omega_i\omega_j}{\omega_i+\omega_j}$ and $a_1=\zeta\frac{2}{\omega_i+\omega_j}$, assuming all the vibration modes of the same damping ratio, ζ. The nth natural frequency of the building with damping is:

$$\omega_{nD}=\omega_n\sqrt{1-\zeta_n^2} \tag{2}$$

where, ω_n is the nth natural frequency of the corresponding undamped building, which can be obtained by solving the eigen value problem:

$$\left[K-\omega_n^2M\right]\phi_n=\mathbf{0} \tag{3}$$

where, ϕ_n is the modal shape vector, and ζ_n is the damping ratio of the nth mode. Before the free vibration tests, the damping ratios of the system is assumed as 3%, which is the suggested value in the current seismic code ([6,18]). The vibration modes and frequencies are computed with Matlab [24] (**Error! Reference source not found.**) and listed in Table 3.

Table 3. Vibration Period (Sec).

Mode #	Matlab		OpenSees		SAP2000	
	Prototype	Scaled	Prototype	Scaled	Prototype	Scaled
1	0.63	0.20	0.63	0.20	0.63	0.20
2	0.22	0.07	0.20	0.06	0.21	0.06
3	0.14	0.05	0.13	0.04	0.13	0.04
4	0.12	0.04	0.11	0.03	0.12	0.03

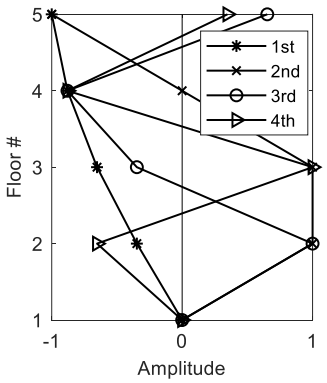

Fig. 3. Vibration modes computed with Matlab

To evaluate the result of the closed-form solution, a 3D FEM was building with OpenSees and SAP2000 [25,26]. In the model in OpenSees, Steel02 material was used for the nonlinear beams and columns where the cross section was discretized into fibers. In the model in SAP2000, line element was used to model the beams and columns. The additional mass was added to each floor level to make sure that the required the similitude law was satisfied [21,22]. The resulting vibration frequencies are listed in Table 3 where the results from the

FEM modes are exactly the same. They are slightly smaller than the ones of the simplified closed-form solution. The error is generally less than 1% indicating that the 4DOF computational model is accurate enough. The 3D model and the resulting vibration modal shapes are shown in Fig. 4, where the 1st, 2nd, and 4th modes are translational, while the 3rd mode is torsional. The modal participation factors of the first two modes are 95% demonstrating that they are the dominant vibration modes [6,18,23].

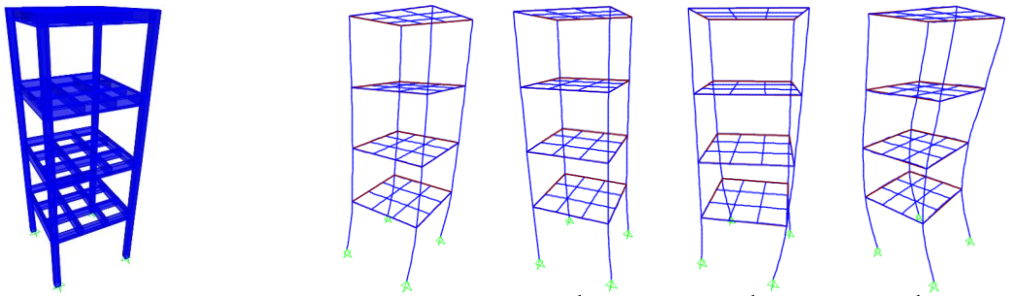

a). 3D model in SAP2000 b). 1st mode c). 2nd mode d). 3rd mode e). 4th mode

Fig. 4. 3D model and vibration modes

3.2 Mass Ratio Effect

The mass ratio (MR) denotes the mass of the equipment divided by the whole mass of the main structure. In ASCE 7-16 [27], it is mentioned that once the MR of the equipment or similar NCs exceeds 25%, they should be designed as a nonbuilding structure instead of NCs because the dynamic interaction cannot be ignored. In the mathematical model, the mass of the equipment is applied to the structure by increasing the magnitude of m_{ei} in Figure 2 at the floors with the equipment. Values of MR range from 5 to 50% with an increment of 5%. The masses are placed on various floor levels as shown in Fig. 2. Same mass ($m_{ei} = m$ in Fig. 2) is placed on each floor if two or more floors are to be assigned, leading to a total of 150 computational cases in Matlab [24]. The stiffness of each story and equipment on each floor is identical i.e., $k_i = k_0$, $k_{ei} = k$ in Fig. 2. Periods computed for various MRs are shown in Fig. 5. In this figure, captions indicate the number of floors that the masses are located at and the legend describe the mass arrangement and which floors the masses are located at. From this figure, one can observe that if the equipment mass is placed on a certain floor level, the vibration period increases with the level of MR (Fig. 5a). A similar trend is observed in the other cases in which the equipment masses are placed on two or more floor levels (Fig. 5b,c). Moreover, if the equipment mass is located on a single floor, the resulting vibration period increases with the floor level of the located mass (Fig. 5a). However, this trend is not observed in the other cases in which masses are placed on two or more floors levels (Fig. 5b,c). For instance, if the masses are placed on the 1st&4th, and 3rd&4th stories (Fig. 5b), the resulting period of the former arrangement is generally larger than the that of the latter. This observation is against the subjective estimation like that shown in Fig. 5a. To solve this issue, a mathematical deduction is carried out to find the distribution character of the period regarding the MR.

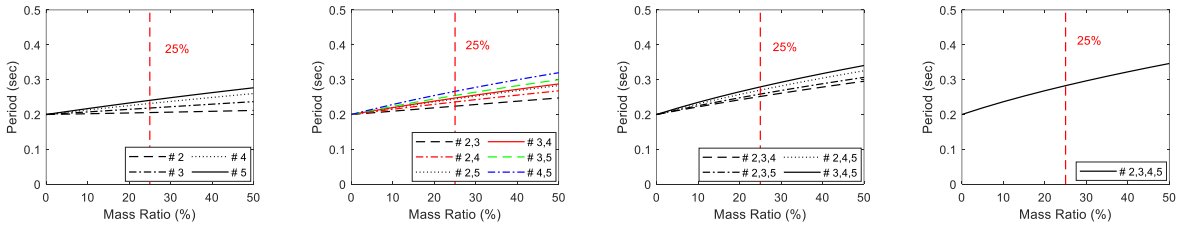

a). One floor b). Two floors c). Three floors d). Four floors

Fig. 5. Period in various mass assignment

The period results from this analytical model are compared against those obtained with OpenSees, and SAP2000 and are shown in Fig. 6, where one can observe that the periods agree with each other well verifying the analytical model developed in Matlab.

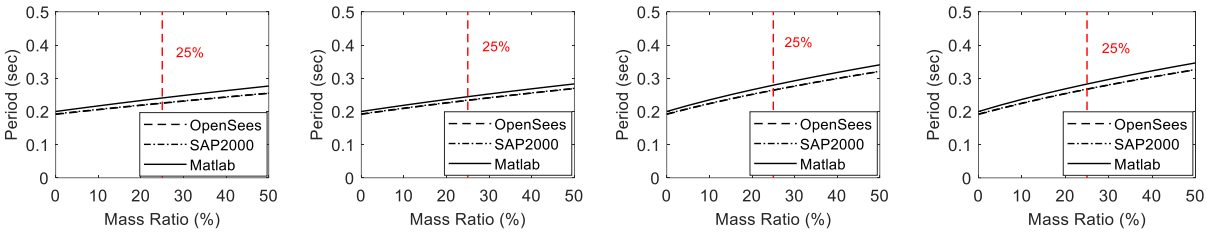

a). Mass in floor # 5 b). Mass in floor # 2,4 c). Mass in floor # 2,4,5 d). Mass in floor # 2 to 5

Fig. 6. Periods of the four DOF structure with equipment mass computed with three methods

4. Free Vibration Test

4.1 Test Setup and Method

The test setup is shown in Fig. 7, where markers and accelerometers were attached to each story level of the frame, which was attached to the strong floor of the lab. The initial condition to initiate free vibration was introduced by applying a small displacement using the string shown in Fig. 7. A Nikon video camera was used to record the whole vibration process. To obtain the displacement response in time history, the recorded videos were processed with digital image computation method. In this test, mass ratios of 20, 25, and 30% were reproduced to evaluate the 25% limit specified in ASCE 7-16 [6].

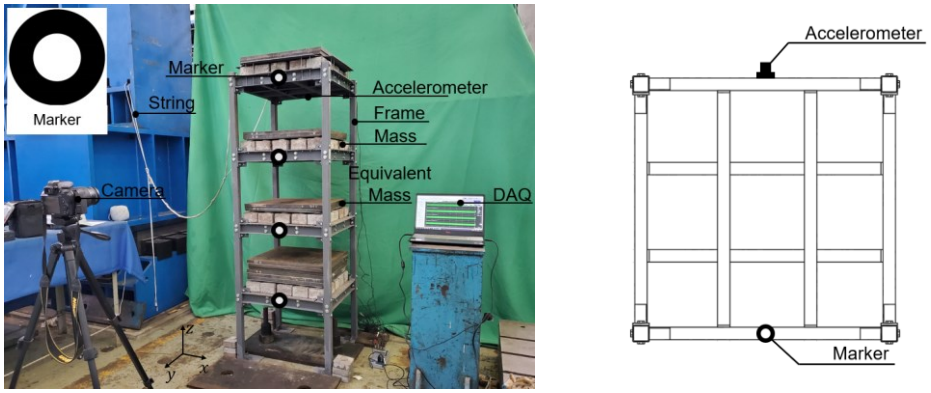

a). Test setup overview b). Layout of the sensors (plan view

Fig. 7. Test setup

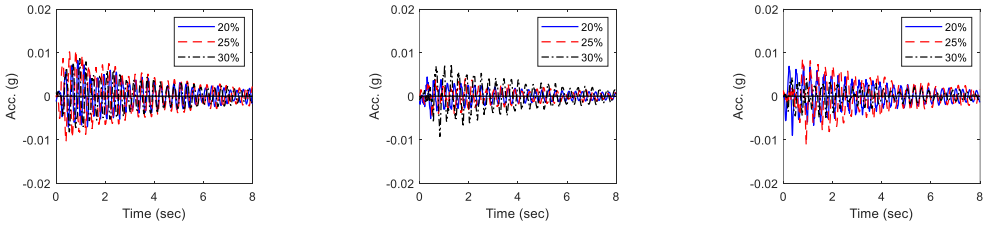

a). Mass in floor # 5 b). Mass in floor # 4,5 c). Mass in floor # 3,4,5

Fig. 8. Acceleration response

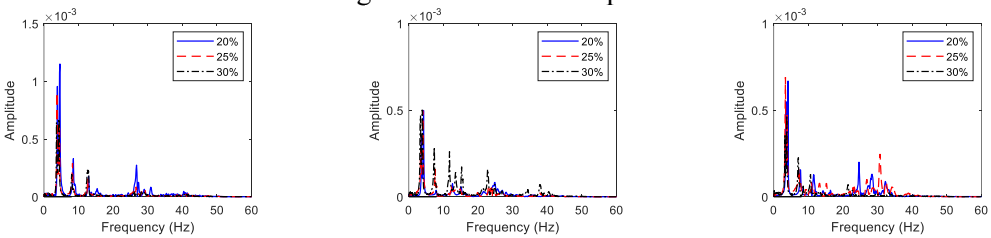

a). Mass in floor # 5 b). Mass in floor # 4,5 c). Mass in floor # 3,4,5

Fig. 9. Fourier Spectra

Table 4. Dynamic Properties.

Mass in Floor #	Mass Ratio	Period (Sec)	Damping Ratio
	20%	0.19	0.95%
# 2	25%	0.20	0.99%
	30%	0.20	0.84%
	20%	0.20	0.95%
# 3	25%	0.21	0.97%
	30%	0.21	0.92%
	20%	0.21	0.79%
# 4	25%	0.21	1.08%
	30%	0.22	0.99%
	20%	0.22	1.10%
# 5	25%	0.23	0.99%
	30%	0.23	0.99%
	20%	0.21	0.93%
# 2, 3	25%	0.21	1.48%
	30%	0.21	1.09%
	20%	0.21	0.83%
# 2, 4	25%	0.22	0.91%
	30%	0.22	0.93%
	20%	0.22	1.00%
# 2, 5	25%	0.23	0.94%
	30%	0.24	0.84%
	20%	0.22	0.74%
# 3, 4	25%	0.23	0.92%
	30%	0.23	1.03%
	20%	0.23	0.82%
# 3, 5	25%	0.24	1.27%
	30%	0.24	1.05%
	20%	0.23	0.79%
# 4, 5	25%	0.25	0.78%
	30%	0.26	1.04%
	20%	0.22	0.99%
# 2, 3,4	25%	0.23	0.93%
	30%	0.24	1.11%
	20%	0.23	0.96%
# 2, 3, 5	25%	0.24	1.11%
	30%	0.24	0.96%
	20%	0.24	1.09%
# 2, 4, 5	25%	0.25	0.96%
	30%	0.26	0.84%
	20%	0.24	1.09%
# 3, 4, 5	25%	0.26	0.96%
	30%	0.26	0.97%

4.2 Test Results

In the conducted tests, equipment mass was placed on 1st, 2nd and 3rd floors. Fig.8 shows the acceleration response histories measured at the 4th floor (Fig. 8). Fundamental natural periods are identified from the Fast Fourier Transform (FFT) of the measured accelerations, Fig. 9. Damping ratio is computed from the FFTs using half power method suggested by Chopra [23]. The computed dynamic properties including vibration frequency and damping ratio are listed in Table 4 and plotted in Fig. 10. The identified values are generally consistent with the results of the numerical analysis (Fig. 10). When the mass is fixed to certain floor levels,

the vibration period and damping ratio increase with the increasing mass ratio. The vibration period increases if a certain amount of mass is evenly disassembled and fixed to two or more floor levels. For the same mass ratio, mass in higher floor levels leads to larger periods and damping ratios.

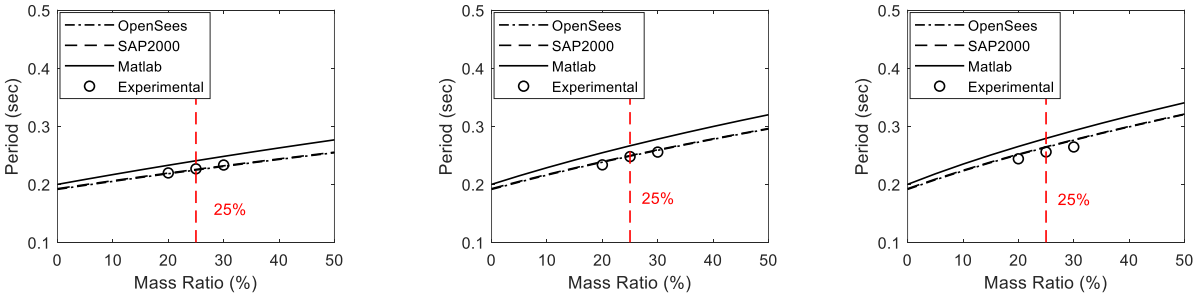

a). Mass in floor # 5 b). Mass in floor # 4,5 c). Mass in floor # 3,4,5

Fig. 10. Fundamental vibration period identified by the experiments and comparison with analytical results

Displacement responses measured at the top of the structure are plotted in Fig. 11, with which, the vibration period of the steel frame was computed and shown in Fig. 12. One can observed that the results obtained from displacement and acceleration responses are almost identical. This observation confirmed the reliability of the experimental and analytical results. The interaction between the equivalent mass and the steel frame exists when the mass ratio even when the mass ratio is smaller than 25%.

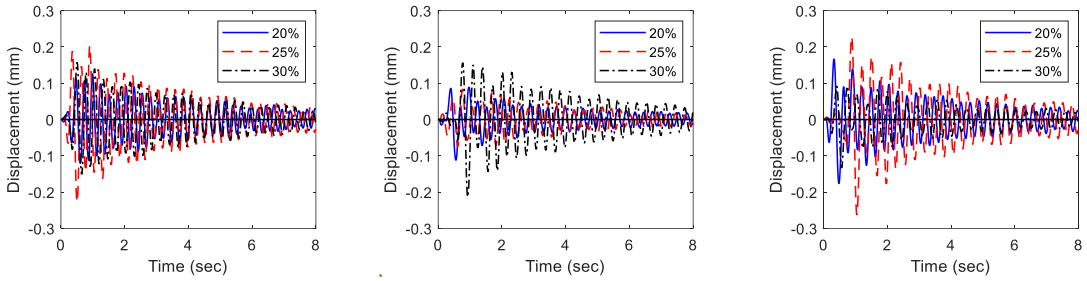

a). Mass in floor # 5 b). Mass in floor # 4,5 c). Mass in floor # 3,4,5

Fig. 11. Displacement response

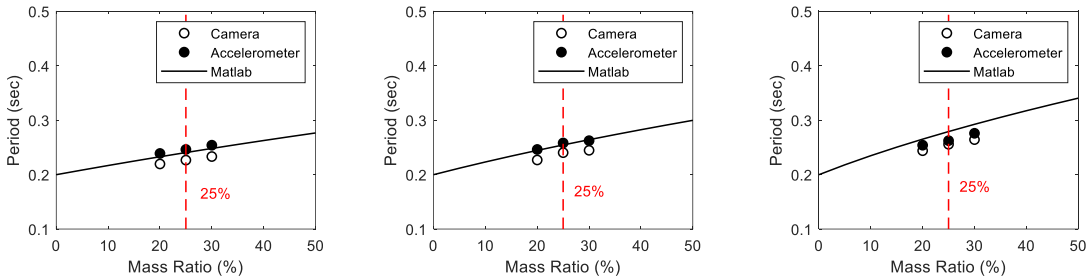

a). Mass in floor # 5 b). Mass in floor # 4,5 c). Mass in floor # 3,4,5

Fig. 12. Period and mass ratio

The relationship between damping and mass ratios are shown in Fig. 13. One can find that when the mass is attached to one floor level, the damping ratio is the largest for the case of the mass placed on the 2nd floor, and smallest for the mass placed on the 3rd floor. Similar trend is found for the case of three masses, while there is no clear trend for the mass located in the other two floors. A general observation is that the damping ratio increases with the mass ratio. The relationship between the damping ratio and the period is shown in Fig. 14 where it is difficult to observe a representative pattern. Similar observations are made from the periods and damping ratios identified from the displacement responses.

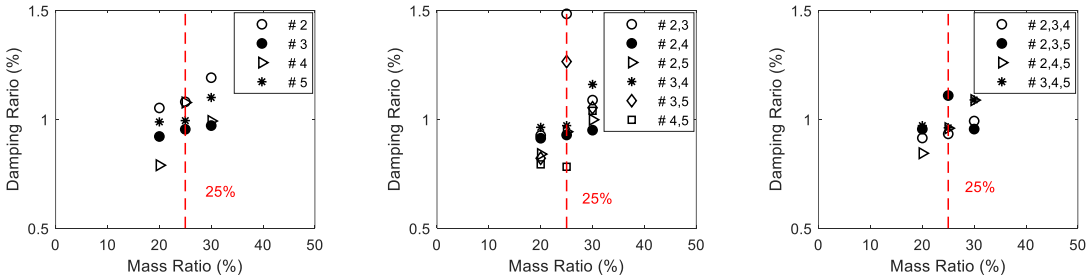

a). Mass in one floor b). Mass in two floors c). Mass in three floors

Fig. 13. Relationship between mass and damping ratios

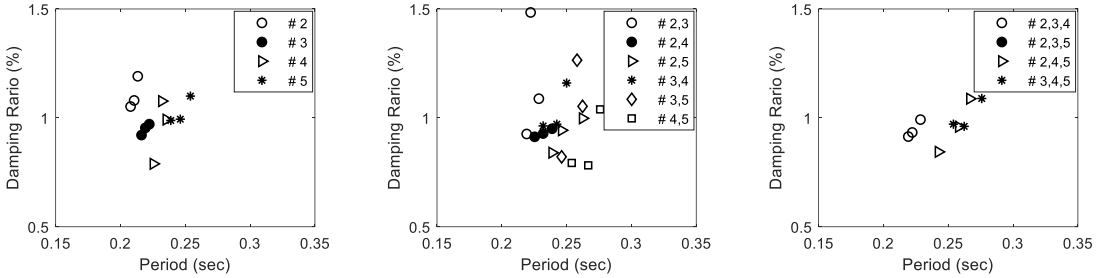

a). Mass in one floor b). Mass in two floors c). Mass in three floors

Fig. 14. Relationship between damping ratio and period

5. Summary and Conclusions

Dynamic interaction between the equipment and the main structure may lead to the damage of both systems if the interaction mechanism is not understood clearly. In an effort to understand this interaction, many analytical studies based on the simplified models of the two systems were conducted. While the influence of the mass ratio on the interaction parameters such as the period and damping ratio is clear, the optimized location of equipment was not investigated comprehensively. In this study, to investigate the seismic interaction in terms of the mass ratio, a 1/10 scaled 4-story steel moment frame was built following according to similitude relations such that the dynamic response of this frame can be related to that of the prototype. The frame was simplified as a four degree-of freedom (4DOF) system to compute its dynamic characteristics. The equivalent masses of the equipment were attached to various floor levels and numerical analyses and free vibration tests were carried out, where some conclusions are listed below:

1) The analytical results with the OpenSees, SAP2000, and the Matlab analytical model agree with each other well. This confirms the accuracy of the simplified MDOF model.

2) The computational and experimental fundamental periods of the steel frame are close to each other. The fundamental period generally increases with the mass ratio. For a certain amount of mass, the corresponding period is larger if located at higher story levels.

3) The fundamental period corresponding to the mass ratios of 20, 25, and 30% do not vary much. Further studies are required to justify the 25% limit in ASCE7-16.

4) The damping ratio of the frame varies between 0.8 to 1.8%, which is different from the 3% value indicated in current code provisions. It increases slightly if the mass is located at higher story levels. The experimental damping ratios should be justified with further analytical and shaking table test studies.

Acknowledgements

The presented research is funded by China National Science and Technology Major Project with grant # 2018YFC0705701, and China National Science Foundation with grants # 51608381, 51578405.

References

[1] Caldwell P, Gatscher JA, and Littler SR (2007). Essential elements of equipment seismic qualification to ASCE 7 by shake table testing, *ASCE/SEI 2007 Structures Engineering Congress*, 16-19 May 2007, Long Beach, CA.
[2] Ayres JM, Sun TY, and Brown FR (1967). *A Report on Non-Structural Damage to Buildings - Alaska Earthquake, March 27, 1964*. National Academy of Sciences, Washington, D.C.
[3] Lew HS, Leyendecker EV, and Dikkers RD (1971). *Engineering Aspects of the 1971 San Fernando Earthquake*. Building Science Series 40, U.S. National Bureau of Standards, Washington, D.C.
[4] Ayres JM, and Sun TY (1973). *Nonstructural Damage, The San Fernando, California Earthquake of February 9, 1971*. National Ocean and Atmospheric Administration, Vol. 1B1(B), Washington, D.C.
[5] California Office of Statewide Health Planning and Development (OSHPD) (1996). *1994 Northridge Hospital Damage: OSHPD Studies: Water, Elevator, Nonstructural*, Office of Statewide Health Planning & Development, Division of Facilities Development, Sacramento, California.
[6] Ding D, Arnold C, Lagorio H, Tobriner S, Rihal S, Mangum R, Hezmalhalch G, Green M, Watson A, Mah D, Metro B, Podany J, and Sharpe R (1990). Architecture, building contents, and building systems. *Earthquake Spectra*, **6**(S1): 339-377.
[7] Goodno BJ, Gould NC, Caldwell PJ, and Gould PL (2011). Effects of the January 2010 Hatian Earthquake on Selected Electrical Equipment. *Earthquake Spectra*, **27**(S1): 1-26.
[8] Miranda E, Mosqueda G, Retamales R, and Pekcan G (2012). Performance of nonstructural components during the 27 February 2010 Chile earthquake. Earthquake Spectra, 28(S1): S453-S471.
[9] Chen Y, and Soong TT (1988). State-of-the-art-review: seismic response of secondary systems. *Engineering Structures,* **10**(4): 218-228.
[10] Villaverde R (1997) Seismic design of secondary structures: state of the art. *Journal of Structural Engineering,* **123**(8): 1011-1019.
[11] Penzien J, Chopra AK (1965). Earthquake response of appendage on a multi-story building, Proc. 5th World Conference on Earthquake Engineering, Volume 2, pp. 476-490.
[12] Igusa T, and Kiureghian AD (1985). Dynamic characterization of two-degree-of-freedom equipment-structure systems. *Journal of Engineering Mechanics*, **111**(1): 1-19.
[13] Igusa T and Kiureghian AD (1985). Dynamic response of multiply supported secondary systems. *Journal of* Engineering *Mechanics*, **111**(1): 20–41.
[14] Igusa T, and Kiureghian AD (1985). Generation of floor response spectra including oscillator-structure interaction. *Earthquake Engineering & Structural Dynamics,* **13**(5): 661-676.
[15] Chaudhuri SR, Villaverde R (2008). Effect of building nonlinearity on seismic response of nonstructural components: a parametric study. *Journal of Structural Engineering*, **134**(4): 661-670.
[16] Segal D, Hall WJ (1989). *Experimental Seismic Investigation of Appendages in Structures*, University of Illinois Engineering Experiment Station, College of Engineering, University of Illinois at Urbana-Champaign.
[17] Lim E, Chouw N (2018). Prediction of the response of secondary structures under dynamic loading considering primary-secondary structure interaction. *Advances in Structural Engineering*, **21**(14): 2143-2153.
[18] Ministry of Housing and Urban-Rural Development of the People's Republic of China (MOUHRD) (2016). *Code for Seismic Design of Buildings. GB50011-2010*, Building Industry Press of China, Beijing, China. (in Chinese)
[19] Krawinkler H (1979). Possibilities and limitations of scale-model testing in earthquake engineering. *Proceedings of the second US national conference on earthquake engineering*. Stanford, pp. 283-292.
[20] Kumar S, Itoh Y, Saizuka K, and Usami T (1997). Pseudodynamic testing of scaled models. *Journal of Structural Engineering*, **123**(4): 524-52.
[21] Liang Z, and Lee G (2006). On similitude law of sub-systems. *Earthquake Engineering and engineering Vibration*, **5**(1): 133-142.
[22] Kim NS, Lee JH, and Chang SP (2009). Equivalent multi-phase similitude law for pseudodynamic test on small scale reinforced concrete models. *Engineering Structures*, 31(4): 834-846.
[23] Chopra AK (2012). *Dynamics of Structures* (4th Edition). Prince Hall, New Jersey, USA.
[24] MathWorks. Bioinformatics Toolbox: User's Guide (R2012a), 2012.
[25] McKenna F, and Fenves GL (2001). *OpenSees Manual*. Pacific Earthquake Engineering Research Center. http://opensees.berkeley.edu.
[26] Computers and Structures. Integrated finite element analysis and design of structures, version 11.0.8. SAP2000, Berkeley, CA, 2007.
[27] American Society of Civil Engineers (ASCE). (2017). *Minimum Design Loads for Buildings and Other Structures, ASCE/SEI 7-16*. ASCE, Reston, Virginia, USA.

